

FEM Analyses on the Influence of Fluid Temperature on the Mechanical Seal Leakage

Andrei Stanciu

Doctoral Student
Petroleum-Gas University of Ploiesti
Faculty of Mechanical and Electrical
Engineering
Romania

Razvan-George Ripeanu

Professor
Petroleum-Gas University of Ploiesti
Faculty of Mechanical and Electrical
Engineering
Romania

A mechanical seal is a dynamic equipment that consists of 2 main pieces, a static ring and a rotating one, that are also having additional auxiliary items such as springs and gaskets. The rotating ring is pushed into frictional contact against the static ring, with the support of springs, fluid pressure, rotational velocity, and other factors. For a minimum leakage value, the forces that are acting on opening the seal must be lower than the those who closing it. A mechanical seal will always leak between the seal face, as it needs lubrication, based on the roughness values. This paper shows how the process fluid temperature plays a very important role in deciding on the mechanical seal behaviour and is calculating the leakage based on different working temperature, considering the gap created by the thermal expansion between the two faces.

Keywords: mechanical seal, fluid temperature, FEM analyses, leakage.

1. INTRODUCTION

Mechanical seals are complex equipment that have the role of lowering the leakage between two surfaces, one static and the other one with rotational movement. By having a frictional contact between the two surfaces, the only way to prevent high wear is to have a fluid film between the two surfaces.

The fluid film can be adjusted based on needs, as for dry gas mechanical seals, different hydrodynamics grooves are used to enhance the fluid film thickness, but with an increase in leakage.

For the fluids considered as high risk, this leakage is not acceptable, and plane faces are used. Those types of faces, have the lowest leakage rate of all, but the highest wear rate as well. The fluid film is controlled, based on the surface roughness and the flatness of the faces. As the thickness of the fluid is less than one μm , a possibility of dry contact is present, which is resolved by choosing the correct pair of materials for the two rings.

Most used paired of materials, for the low leakage mechanical seals are soft against hard faces, with the soft one being represented by carbon impregnated with resins, while the hard face is typically considered as silicon carbide or tungsten carbide.

Another possibility of material pair will be hard against hard, which typically two rings of tungsten carbide are used, but when the fluid film is considered, no contact between the two rings needs to be taken into contact [1].

Different studies analyzed the mechanical seal temperature changes, and tried to improve the cooling using different methods, one being presented by A. Gidden [3] in his work, which showed the influence of the temperature increase at the mechanical seal body,

and ways of improving the cooling of mechanical seals by changing the design with a fin mating ring. His analysis showed improved cooling on the updated design. I. Etison et al., [3] or X.Q Yu et al. [4], showed the influence of laser-textured mechanical seals on better lubrication and cooling, but with the increase of hydrodynamic forces in the interstition between seal faces resulting in the increases of leakage. L. K. Chauhan [5] showed the influence generated by a different type of material than the standard ones used on the mechanical seal heat thermal transfer. Additionally, to the mechanical seal analyses, other areas have tried to deal with the generated temperature by improving the heat transfer, such as works of N. A. Ahmad [6] and Rama Ganesh R [7], by using nano lubricants on improving the durability on bearings.

Previous literature focuses mainly on the temperature generated by the friction between the two faces in contact, where factors such as surface roughness and fluid film pair have a significant effect on the obtained values. Lately, materials with roughness equal to one light band have been developed, resulting in some special mechanical seals being able to run in dry conditions [8].

The paper is focused on an existed mechanical seal type CDSA, which stands for cartridge double seal arrangement. This equipment, is internal pressurized, with a second fluid being inserted on the mechanical seal, creating a barrier for the process fluid, to not leak, but also supports with cooling down the components. Main objective is concentrated on creating a validated mathematical model, by standard, which can explain the thermal behavior of the equipment, under different process fluid temperatures.

The results show the change of the contact pressure behavior on a mechanical seal, including the influence of temperature on leakage, during operational and start-up. The contact pressure between the two faces is directly affected by the temperature increase, with a maximum pressure increased by 24 times and a leakage rate of 15 times, when is considered process fluid temperature from 22°C to 200°C .

Received: January 2025, Accepted: March 2025

Correspondence to: Prof.Dr.Eng. Razvan George Ripeanu, Petroleum-Gas University of Ploiesti, Blvd. Bucuresti 39, 100680 Ploiesti, Romania
E-mail: rrapeanu@upg-ploiesti.ro

doi: 10.5937/fme2502212S

© Faculty of Mechanical Engineering, Belgrade. All rights reserved

FME Transactions (2025) 53, 212-224 212

2. CALCULATION

The mechanical seal design varies from one case to another, but the construction of a common seal can be found in figure 1.

The working mechanism of a mechanical seal consists in two rings (called also primary seals), one static and one rotating that are being kept in contact with the support of a spring load. The rotating ring that is connected to the sleeve, is being granted a rotational movement, creating a frictional contact between itself and the static ring. Additionally, secondary sealing elements, such as O-rings and other elastomers are used to provide sealing and help compensate for any misalignment or minor imperfection of the primary seal faces.

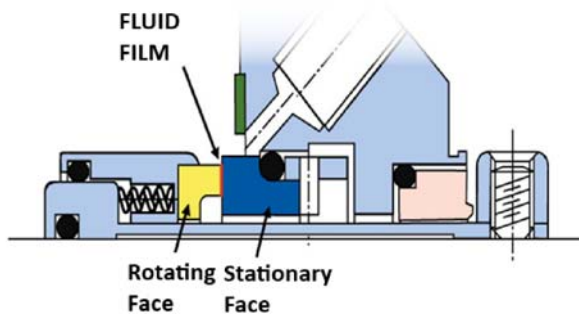


Figure 1. Mechanical seal construction, [8]

For the leakage between the two faces to stay minimalistic, the forces that are acting on the seal to close needs to be lower than the ones acting to open the mechanical seal, but this will not eliminate completely the leakage, as some fluids will regardless leave the equipment through the roughness surfaces of the faces. For mechanical seals that demands a greater value of fluid film thickness, the opening force will surpass the value of the closing force, but with significant more leakage. At some point, the opening and closing forces will balance themselves with the support of spring load. The aim of this paper is to analyse the thermal characteristics of the mechanical seal, thus we must begin with the heat generated by the frictional contact, a value that can be taken from API 682 [9]. Those calculated values will be required for both thermal and static analysis later into the paper.

$$H = \frac{T_r \cdot N}{9550}, [\text{kW}] \quad (1)$$

$$T_r = p_c \cdot A \cdot f \cdot \frac{D_m}{2000}, [\text{N} \cdot \text{m}] \quad (2)$$

$$p_c = \Delta p \cdot (B - K) + p_{sp}, [\text{MPa}] \quad (3)$$

$$A = \frac{\pi \cdot (D_o^2 - D_i^2)}{4}, [\text{mm}^2] \quad (4)$$

K , is a number between 0 and 1 which represents the pressure drop as the sealed fluid migrates across the seal faces. For flat seal faces (parallel fluid film) and a non-flashing fluid, K it is approximately equal to 0.5, [9]. For convex seal faces (converging fluid film) or flashing fluids, K it is greater than 0.5, [9]. For concave seal faces (diverging fluid film), K it is less than 0.5, [9].

The balance ratio value representation it is showed in the Figure 2, and the values could be calculated with relations (5.a) and (5.b) [9];

For external pressured seals (where the external pressure is higher than the barrier fluid), B it is:

$$B = \frac{D_o^2 - D_b^2}{D_o^2 - D_i^2} \quad (5a)$$

$$B = \frac{D_b^2 - D_i^2}{D_o^2 - D_i^2} \quad (5b)$$

For internal pressured seals (where the barrier fluid pressure is higher than the pump fluid pressure), B it is:

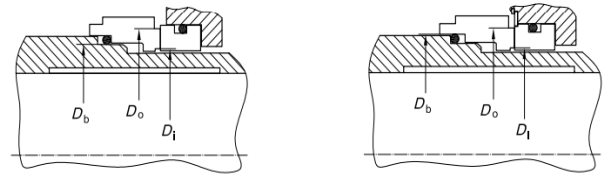


Figure 2. Balance ratio measurement points, [9]

From (3), all the factors are dimensional or process base, the only missing component will be spring pressure.

The principle to find the spring pressure is by starting to understand the three main components that act on the seal [10]:

$$F_t = F_h - F_c + F_{sp}, [\text{N}] \quad (6)$$

Spring force, must have a value higher than the friction force, considering the mechanical seal in stand by condition, $F_h = 0$.

To determine the friction force between the two entities, we are going to use the (7), given by Parker [11].

$$F_c = f_c \cdot L \quad (7)$$

Friction coefficient value is taken from Parker 5-9 Figure, while the length from table 5-4 [11].

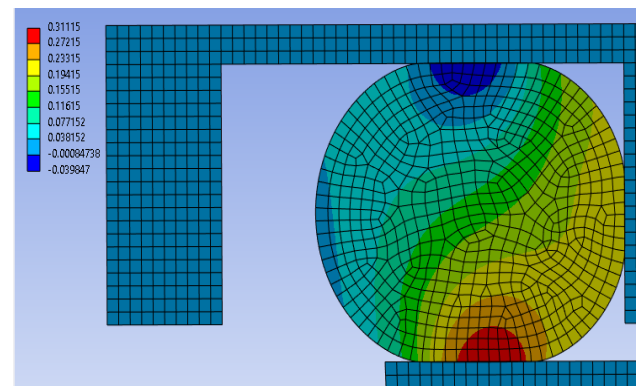


Figure 3. O-Ring compression

Figure 3 was created to determine the compression of the mechanical seal, as it was needed for the value of the friction coefficient. This can be obtained also analytical, with the (8).

$$C = \frac{A_0 - A_d}{A_0} \cdot 100, [\%] \quad (8)$$

With the friction force obtained, we need to calculate the spring force required to overcome this action. The spring force is represented by (9).

$$F_{sp} = -k \cdot x, [N] \quad (9)$$

$$k = \frac{G \cdot d^4}{64 \cdot N_s \cdot R^3}, \left[\frac{N}{mm} \right] \quad (10)$$

Almost all of the primary mechanical seal walls are in contact with the process or barrier fluid, as presented in the figure 4. Due this, all the surfaces convection values will be calculated, as per figure 5.

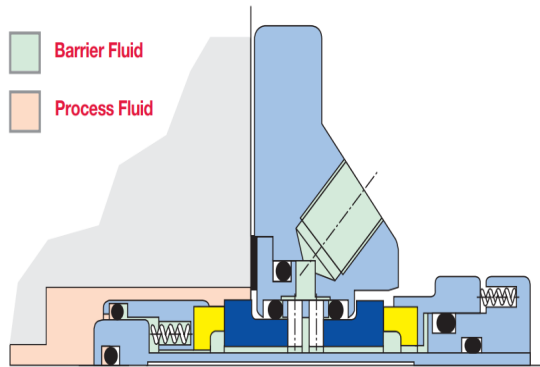


Figure 4. Fluid acting on the CDSA mechanical seal, [8]

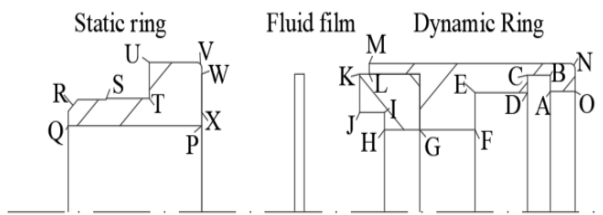


Figure 5. Convection surfaces on the primary seal, [8]

1. Surface of points RS, ST and UT.

Those surfaces, not being in contact with any liquid will not be taken into consideration for the analysis, as the convection is done with air in a free status, resulting a very small value convection value [12,13].

2. Boundaries AO. BC, DE, FG, GH, HI, KL, MN [12,13].

The above-mentioned surfaces are represented by the horizontal faces that are getting in contact with the barrier or process fluid, from the rotating ring.

$$h_r = \frac{0.135 \cdot k_f \cdot \left[\left(0,5R_c^2 + 2 \cdot Re_a^2 \right) \cdot Pr \right]^{0.33}}{D_r} \quad (11)$$

$$Re_c = \frac{\omega \cdot D_r^2}{\nu} \quad (12)$$

$$Re_a = \frac{U \cdot D_r}{\nu} \quad (13)$$

$$\nu = \frac{\mu}{\rho} \quad (14)$$

3. Boundaries PQ and UV [12,13].

Entities that are part of this group, are similar with the ones from point two, with the difference being that those areas are part of the static ring.

$$h_s = \frac{0.115 \cdot k_f \cdot Re^{0.8} \cdot Pr^{0.4}}{S_s} \quad (15)$$

$$Re = \frac{2 \cdot V \cdot S_s}{\nu} \quad (16)$$

4. Surfaces AB, CD, EF, HI, LM, NO, PX, RQ and VW [12,13].

Those domains are represented by the vertical faces that are getting into contact with the barrier or process fluid, including the interstitial surface.

$$h_v = \frac{0.664 \cdot K_f \cdot Re_v^{0.5} \cdot Pr^{\frac{1}{3}}}{L_w} \quad (17)$$

$$Re_v = \frac{V_v \cdot S_v}{\nu} \quad (18)$$

In figure 6 are presented the measured dimensional characteristics of the primary seal component of the mechanical seal type CDSA analyzed.

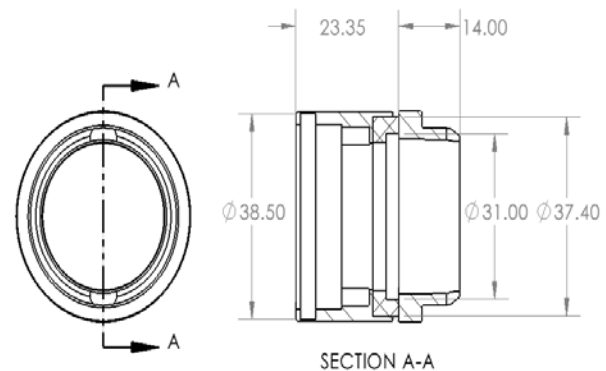


Figure 6. Inboard seal dimensions

Material pair for this mechanical seal, has been chosen by the manufacturer to be carbon impregnated with resins for the contact surface of the rotating ring, while for the static ring was considered silicon carbide. To be mentioned that the rotating ring, is composed of two materials, the previous mentioned for the contact surface, while the body is from 316L SS.

The properties of the pair of materials can be found in table 1. 316L SS and SiC materials are considered from Ansys Discovery [14] data base, while the information for carbon impregnated with resins are taken from supplier directly.

On table 2 are presented the fluid parameters for this scope, with the information regarding the process fluid considered from [15].

Table 1. Material properties

Parameter	Material		
	316 L SS	SiC	C
Density [kg/m ³]	7970	3100	1800
Tensile Yield Strength [MPa]	230	390	45

Tensile Ultimate Strength [MPa]	521	390	45
Poisson's Ratio	0.27	0.14	0.2
Young's Modulus [GPa]	195	410	24
Isotropic Thermal Conductivity [W/m·°C]	14.2	110	8
Coefficient of Thermal Expansion [1/°C]	1.61E-05	2.69E-06	4.7E-06

Table 2. Fluid properties

Parameter	Barrier fluid	Process fluid			
	22 °C	40 °C	100 °C	150 °C	200 °C
Density [kg/m ³]	998	721	681	628	570
Specific heat [kJ/Kg·°C]	4.18	2.2	2.46	2.74	3.04
Dynamic viscosity [10 ⁻⁴ Ns/m ²]	9.5	3.70	2.25	1.56	1.11
Thermal conductivity [W/m·°C]	0.606	0.11	0.10	0.09	0.08

For the calculation, all the working and dimensional parameters required are presented in Table 3.

Table 3. Dimensional and working parameters

Description	Value
Working fluid pressure	0.3 MPa
Barrier fluid pressure	0.44 MPa
Pump shaft speed	3000 RPM
Outside diameter of the seal, D_o	37.4 mm
Inside diameter of the seal, D_i	31 mm
Balance diameter of the seal, D_b	38.5 mm
Pressure drop coefficient, K	0.5
Number of springs, n	6
Shear modulus, G	78600
Spring wire diameter, d	0.5
Number of spires, N_s	13
Average radius of the spring, R	1.11
Spring diameter, D_{sp}	2.72

Based on the (1) to (10), we can calculate all the required parameters with results being presented on table 4.

For the friction value caused by the deformation between the O-Ring and the body of the seal, values are from Parker 2-127 seal table [11], with a friction due to O-ring compression of 0.0125 kgf/mm, and a length of rubbing surface around 114.554 mm.

Table 4. Calculation of parameters

Parameter	Value
Area, A	343.64 mm
Seal balance ratio, B	1.19
Friction force, F_c	14.04 N
Spring force per one-unit $F_{sp,l}$	2.34 N
Spring constant, k	4.4361 N/mm
Spring displacement, x	0.5276 mm
Spring displacement including wear, x_w	1.877 mm
Spring force per unit, considering wear	8.33 N

$F_{sp,l,f}$	
Total spring force considering wear, $F_{sp,f}$	49.96 N
Spring pressure, p_{sp}	0.14539 MPa
Contact pressure, p_c	0.242 MPa
Running torque, T_r (dry)	0.240 N·m
Generated heat, H (dry)	0.0754 kW
Running torque, T_r (lubricated)	0.0995 N·m
Generated Heat, H (lubricated)	0.312 kW

We require a total compression of 0.5276 mm for the seal to overcome the friction force, but we need to consider the wear of the carbon impregnated with resins as well. For the mechanical seal to achieve the end of the life, the material of the carbon face needs to wear out. This surface has a dimension of 1.35 mm, that will be added to the 0.5276 mm. This addition is for the spring value to always have more force than the friction force.

As presented in table 4, the lubrication regime has an impactful role on the heat which is generated due to frictional contact between the two faces, as the friction coefficient will vary, the heat generation and wear will increase.

3. EXPERIMENTAL DETAILS AND RESULTS

For the determination of the friction coefficient, different experiments have been conducted. The tests were made on a CSM tribometer, model TRB, found in figure 7.

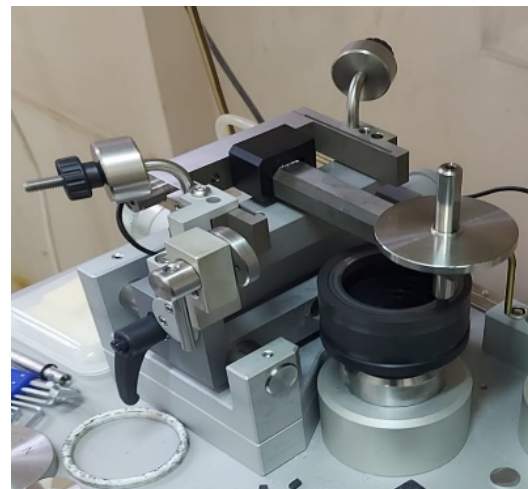


Figure 7. CSM tribometer, model TRB

The role of the equipment is to determine the friction coefficient between the carbon impregnated with resins and silicon carbide material combination. For the experiment, one ring of silicon carbide was considered as a disk type sample which had a rotational movement of 0.5 m/s, that got in contact with a fixed cube shape probe (3.96 x 3.96 x 4 mm), which has a flat face. A force of 3.5 N was used to obtain a similar contact pressure as the one calculated in table 4. The experiment can be seen in the figure 8.

The parameters of the experiment are presented on the table 5. Results of the experiment can be found in figure 9, with the friction coefficient considered 0.1689, a number around which the values tend to stabilize. The obtained stabilized value of COF was used at calculus obtained and presented in table 4.

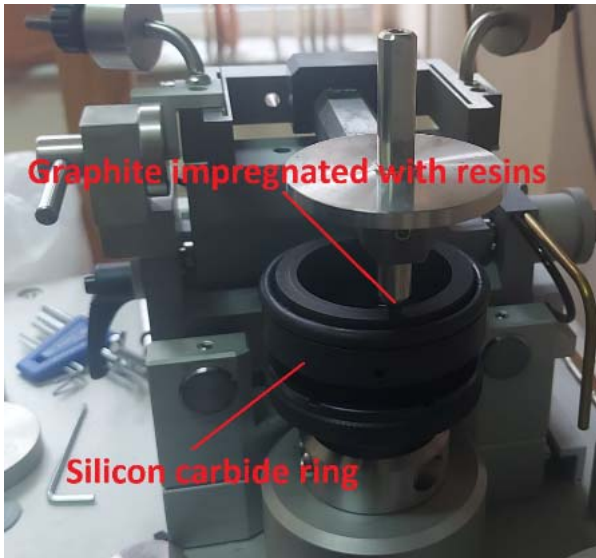


Figure 8. SiC ring mounted on CSM tribometer

Table 5. CSM tribometer working parameters

Parameter	Value
Radius	29 mm
Speed	0.5 m/s
Ambient Temp.	29 °C
Friction length	400 m
Acquisition rate	2.7 Hz
Material 1	Carbon impregnated with resins
Material 2	Silicon Carbide
Contact force	3.5 N
Lubrication	Dry

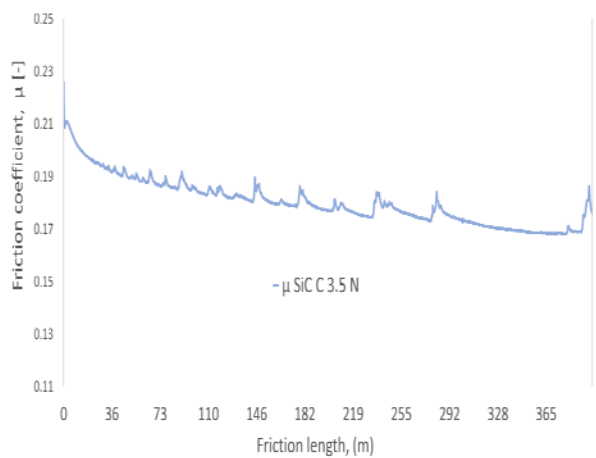


Figure 9. Values of COF vs. friction length

The presence of the spikes in the above graphic are a cause of the dry running of the mechanical seal, resulting in wear.

On parallel with the friction coefficient determination, a thermal measurement took place, by measuring the heat generated by the friction with the support of a FLIR-50 thermal camera, which can be found in the figure 10. As the ambient temperature at the measurement time was around 13°C, and the temperature measurement being presented in the figure 10 as 17.5°C, it results in a temperature increase of 4.5°C. If we use the above calculation from chapter two, it will result that for a 327 RPM, we will have a heat flux of 0.007585 kW, while for the 3000 RPM as in real

conditions the shaft works, the resulting heat flux will have a value of 0.069587 kW.



Figure 10. FLIR-50 measurement of temperature



Figure 11. C – SiC generated temperature

4. FINITE ELEMENT ANALYSIS

The inboard mechanical seal is going to be analyzed using ANSYS Static Structural shown in figure 12, but also thermal. The fluid domain is going to be calculated using the Ansys Fluent.

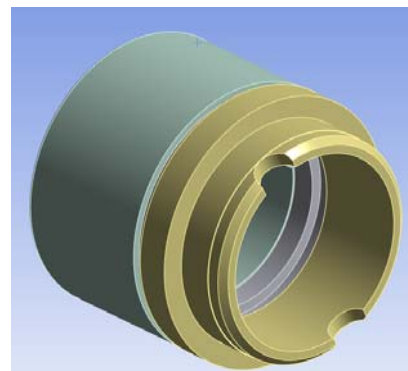


Figure 12. Inboard seal model

The system is having two types of contacts:

1. Contact between the 316L SS body, and the carbon impregnated with resins body (Figure 13).

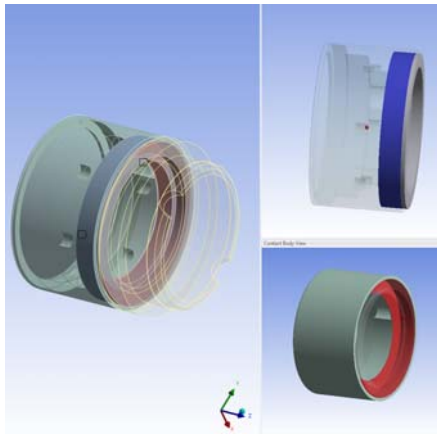


Figure 13. Bonded contact inside the rotating ring

Due to economical and structural reasons (carbon impregnated with resins being a brittle material), the rotating ring is being composed out of two materials, as stated before. Those two materials are being bonded together but due to their different properties (such as Poisson ratio, thermal expansion etc.), they are not able to sustain high pressures / temperatures. This combination has been considered as bonded contact into the analysis.

2. Contact between the rotating ring and the static ring (Figure 14).

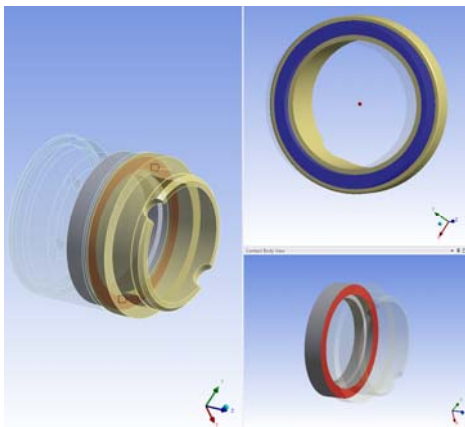


Figure 14. Frictional contact between the static and rotating ring

This contact represents the friction between the two rings, and is represented with a frictional contact.

The friction coefficient between the two rings has been calculated on the previous chapter for the dry running, while for the lubricated situation, a 0.07 [16] value was considered.

A test run took place for different mesh values, where the results variation was considered. For meshes higher than 0.7 mm of the contact surface, the contact pressure value will have a value with ~15% higher than the 0.6 mm. After lowering the values up to 0.1 mm, the results will be very similar between 0.6 and 0.1 mm, but with a running time of 13 times higher. In total, more than 30 tests were conducted, under different mesh values, with the values from table 6 being considered the best fit.

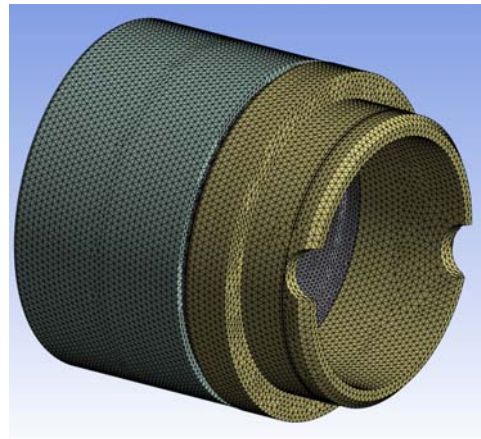


Figure 15. Inboard seal discretization

Table 6. System discretization

Parameter	Value
Dynamic ring body mesh	0.8 mm
Dynamic ring contact body mesh	0.5 mm
Static ring mesh	0.8 mm
Refinement on both contact surfaces	Level 2
Refinement on spring acting surface	Level 1
Mesh Type	Hex Dominant Method All Quad
Elements	988229
Nodes	1438509

The loads and supports used for the analysis depend on the stage of running, as a mechanical seal has three stages:

1. The Stand-by situation, when only the spring force is acting on the mechanical seal. On this situation, the seal is transported or mounted on the pump shaft.

For this case, the contact shall be calculated with (3), but, as no fluid is present into the seal, $\Delta p = 0$, resulting the contact pressure will be equal with the spring pressure. The spring pressure is being given by the 6 springs that the manufacturer used into the design. The values of each spring were calculated, and it is presented on table 4. The inboard load on spring on stand-by is shown in figure 16.

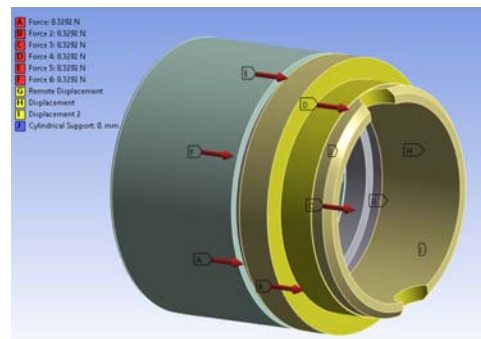


Figure 16. Inboard load on stand-by

2. Before starting the pump, the barrier fluid shall be inserted into the mechanical seal, thus adding the internal pressure, as presented into the figure 17. The barrier fluid will act on all components as shown in figure 4.

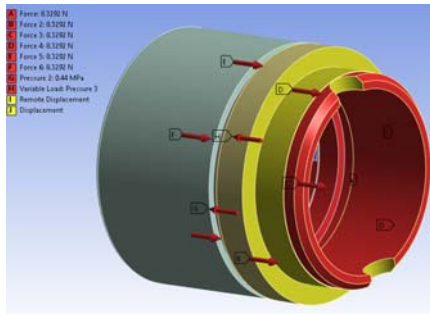


Figure 17. Inboard load on pre-start, considering barrier fluid component

The Δp value from (3), will be equal with 0.44 MPa, resulting a contact pressure equal with:

$$p_c = \Delta p \cdot (B - K) + p_{sp} = 0.449, [\text{MPa}]$$

The component that is working on opening the mechanical seal is represented by the interstitial pressure. This pressure is being given by the fluid film which is lubricating the seal, and its pressure behavior has been calculated with the support of Ansys Fluent, with the results presented in figure 18. This distribution has been obtained by choosing the laminar viscous model [17] ($Re < 2300$, based on (18)), with the dimensions being identical with the contact surface between the rotating and stating rings. System is being considered as converged when the residuals equal to 10^{-6} , and with a mesh value equal of $0.1 \mu\text{m}$ (maximum value converged by the software). The geometry utilized was a tube with D_i and D_o values presented in table 3, and a thickness equal with $0.1796 \mu\text{m}$.

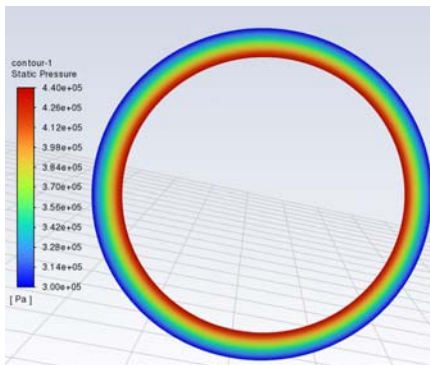


Figure 18. Interstitial pressure

Figure 18 has been realized considering the parameters from the case 3, but we can remark that the pressure distribution is linear. Instead of 0.3 MPa on the outlet, the value is considered as 0 MPa, with an inlet of 0.44 MPa. The thickness of this interstitial pressure is the same order as the magnitude of the combined surfaces roughness of the primary and the mating ring [18].

$$R_c = \sqrt{R_p^2 + R_m^2} \quad (19)$$

Using (19) and considering a value of $0.127 \mu\text{m}$ for both primary and mating ring, it will result a total roughness, and a gap of $0.1796 \mu\text{m}$.

3. The working condition, when the pump is functioning, adding the pressure of the process fluid and

rotational speed, we obtain the inboard loads presented in figure 19.

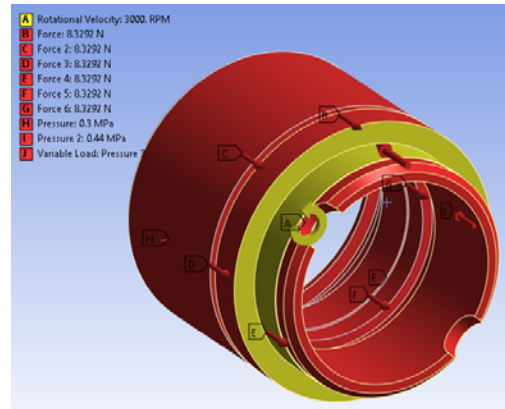


Figure 19. Inboard load on working conditions

The interstitial pressure is having the values presented on the figure 18.

The information required from the static analysis is the contact pressure, necessary to calculate the heat flux resulted due to frictional contact.

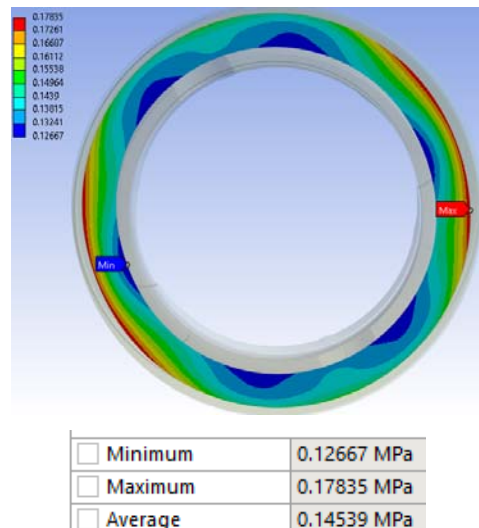


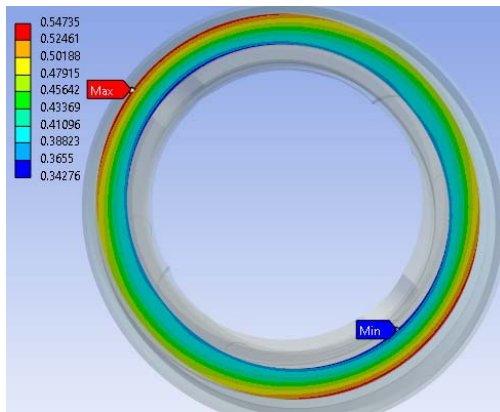
Figure 20. Inboard contact pressure on stand-by

In figure 20 is presented the contact pressure obtained on stand-by conditions.

The contact pressure patterns are created due to material deformation, as an effect of the spring force. The contact pressure resulted analytical is identical with the one resulted from the FEA (average results).

For the second case, the fluid pressure is having a significant impact, but as the barrier fluid is closing the seal due to unbalanced status ($B > 1$), we can see the impact on the figure 21. An imbalanced mechanical seal is having a higher contact pressure. As it is using more energy to close the seal, the friction, heat and wear created are going to increase, resulting in a lower working period. Those seals are not recommended on being used for high pressure or high temperature scopes, as we can see later into the paper.

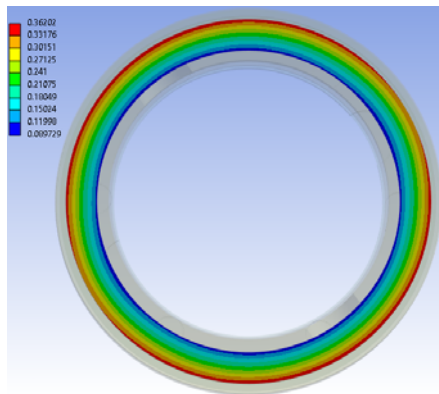
By adding the two pressure components, we have a difference between analytic and FEA results of $\sim 2.3\%$. This is based on the material behavior, as the deformations are not considered into (3).



Minimum	0.34276 MPa
Maximum	0.54735 MPa
Average	0.43843 MPa

Figure 21. Inboard contact pressure, considering barrier fluid component

Based on the above two situations, we can confirm the model to be correct, FEA matching the analytic values. Our attention is on case 3, where the working conditions are meet.



Minimum	8.9729e-002 MPa
Maximum	0.36202 MPa
Average	0.22579 MPa

Figure 22. Inboard contact pressure on working conditions

The difference between FEA and analytic is at 6.6%, with the standard contact pressure being higher. The information required from this analysis is the contact pressure distribution.

While considering no thermal influence, the contact pressure is being shared across the contact section, but with an increase of wear on the outside diameter due to pressure discrepancy between the barrier fluid and the process fluid. This situation is close to impossible, as the friction between the two seals will generate heat, so thermal deformation will occur. With this information, we can create heat flux, using (1), but instead of one point, we can calculate it for the entire distribution, resulting in the distribution from figure 23. The friction coefficient considered for the running was the one from lubricated case (0.07).

For checking the influence of the process fluid temperature on the mechanical seal behavior, we are going to consider the fluid at four different temperatures, with parameters presented on the table 2.

Using (11), (15) and (17), we can calculate the convection of the fluid with the seal surfaces, values presented on table 7.

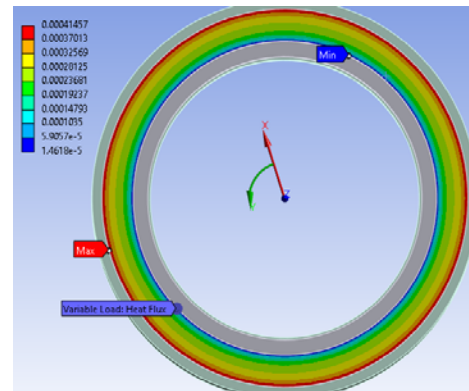


Figure 23. Heat Flux distribution

Table 7. Convection values [W/mm²·°C]

Area	Barrier fluid	Process Fluid				
		22°C	40°C	100°C	150°C	200°C
AB		0.0055	0.0058	0.0054	0.0052	
BC	0.0142					
CD	0.0425					
DE	0.0141					
EF	0.0235					
FG	0.0153					
GH	0.0151					
HI	0.0450					
IJ	0.0151					
KL		0.0016	0.0018	0.0018	0.001	
LM		0.0034	0.0036	0.0034	0.0032	
MN		0.0016	0.0018	0.0017	0.0017	
NO		0.0043	0.0051	0.0048	0.004	
AO		0.0016	0.0019	0.0018	0.0018	
PQ	0.0035					
QR	0.0345					
RS	0.0035					
UV		0.0007	0.0009	0.0009	0.0009	
VW		0.0034	0.0044	0.0041	0.0039	
PX	0.0422					

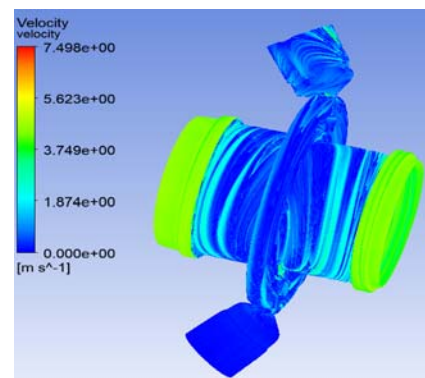


Figure 24. Velocity inside the CDSA mechanical seal

To determine the velocity inside the mechanical seal, a CFD model has been created, using the CDSA model, with a mesh of 0.15 mm, resulting in 2671645 nodes and 13603358 elements. The mesh was considered as the minimum value when the system will converge. Based on the Reynolds numbers calculated with (12), (13), (16),

and (18), with majority of the values being higher than 9000, it results in a turbulent flow, so the viscous model k-omega SST has been selected with 600 iterations, having the results showed in figure 24 [19].

Considering information from table 7 and figure 23, we can see the effect of different fluid temperatures on the mechanical seal surface temperatures.

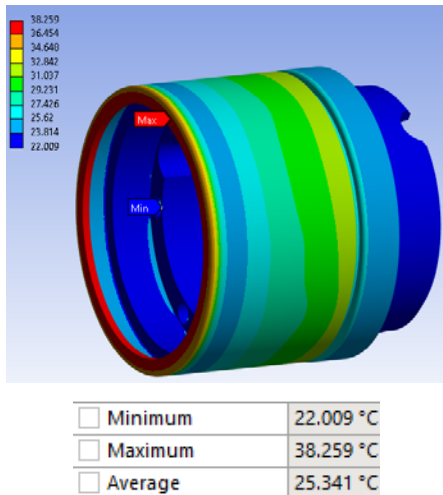


Figure 25. Inboard seal temperatures considering 40°C on process fluid

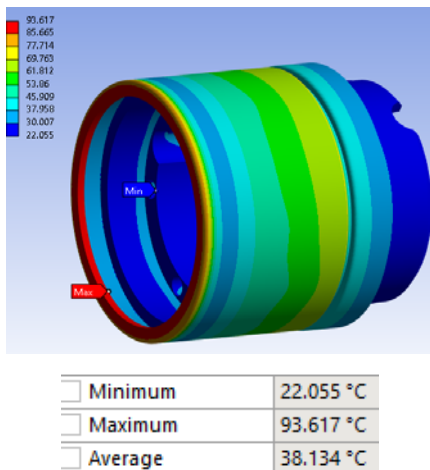


Figure 26. Inboard seal temperatures considering 100°C on process fluid

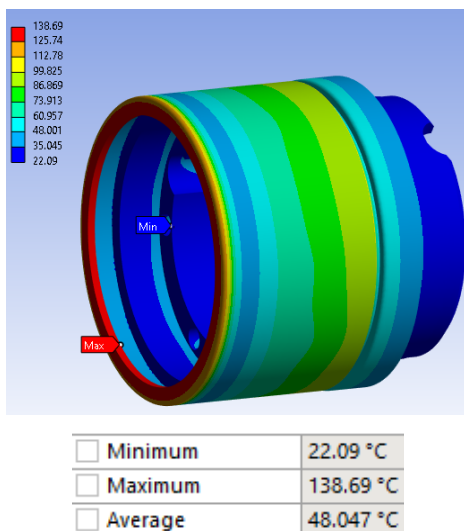


Figure 27. Inboard seal temperatures considering 150°C on process fluid

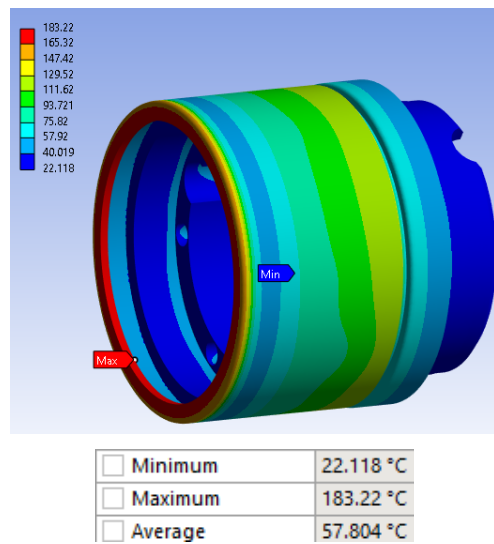


Figure 28. Inboard seal temperatures considering 200°C on process fluid

From the four cases, we can see the flux of barrier fluid is enough to cool down the seal, considering an ambient temperature of 22°C, as the minimum temperature of 22.1°C is presented inside the mechanical seal, but also outside of the static ring.

The maximum temperature results on the back of the equipment, where the barrier fluid is not present due to O-Ring sealing. On the outside of the seal shell, where the process fluid is in direct contact, we have an increase in temperature, but having a thin wall, the thermal conduction will take place, and the wall will be cooled down by the fluid barrier. As expected, where the carbon impregnated with resins component is located, the temperature is increasing, as the thickness of the wall increased, lowering the heat transfer.

With the Static-State Thermal analysis completed, it is going to be imported on the static structural module, resulting in the influence of both mechanical and thermal.

We can construct the final model and analyses the behavior of the mechanical seal under different temperatures. For this, we will observe the deformations, due to thermal and mechanical loads combined.



Figure 29. Deformations for a process fluid temperature of 22°C (scale of 1:390)



Figure 30. Deformations for a process fluid temperature of 40°C (scale of 1:620)

As expected from the figures 25-28, the most deformed surface will be the rear side, as on that area,

the temperature has the highest value. Proportionally with the temperature increase, the deformation is following as well, the contact between the two surfaces will change from a well-rounded contact to a low area contact, how can be seen on Figures 30-33. The contact surfaces between the two rings are diminished, resulting in an increase in contact pressure. With higher contact pressure, the temperature generated by the frictional contact and wear will increase. This will create non-uniform wear, until the seal will stabilize. This stabilization will remain, until one of the working parameters of the mechanical seal will change, resulting in another non-uniform wear period. Those periods are dangerous for mechanical seal durability, as material will be lost in process, resulting in a non-uniform profile which can lead to failure.

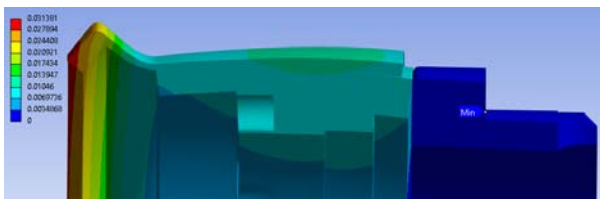


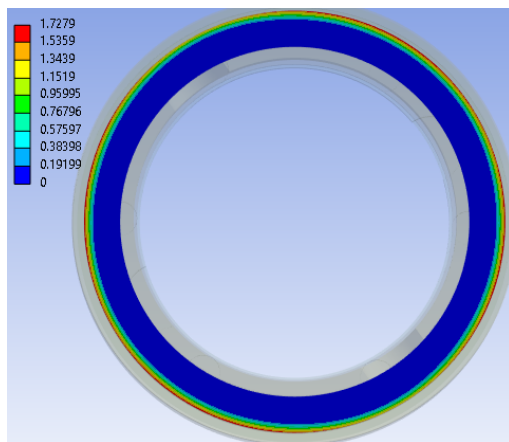
Figure 31. Deformations for a process fluid temperature of 100°C (scale of 1:140)



Figure 32. Deformations for a process fluid temperature of 150°C (scale of 1:87)

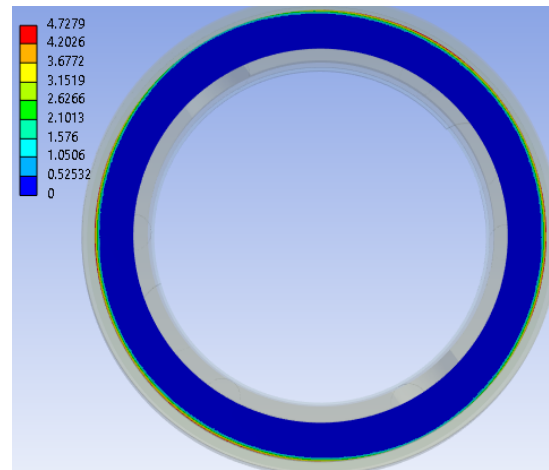


Figure 33. Deformations for a process fluid temperature of 200°C (scale of 1:63)



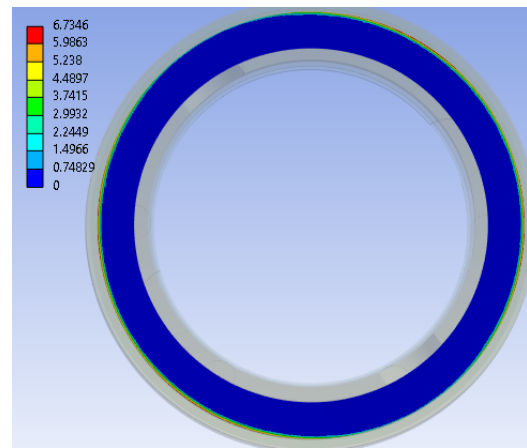
Minimum	0. MPa
Maximum	1.7279 MPa
Average	0.26233 MPa

Figure 34. Contact pressures for a process fluid temperature of 40°C



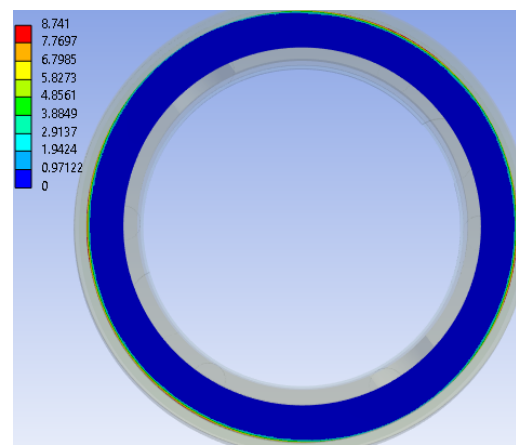
Minimum	0. MPa
Maximum	4.7279 MPa
Average	0.30834 MPa

Figure 35. Contact pressures for a process fluid temperature of 100°C



Minimum	0. MPa
Maximum	6.7346 MPa
Average	0.36006 MPa

Figure 35. Contact pressures for a process fluid temperature of 150°C



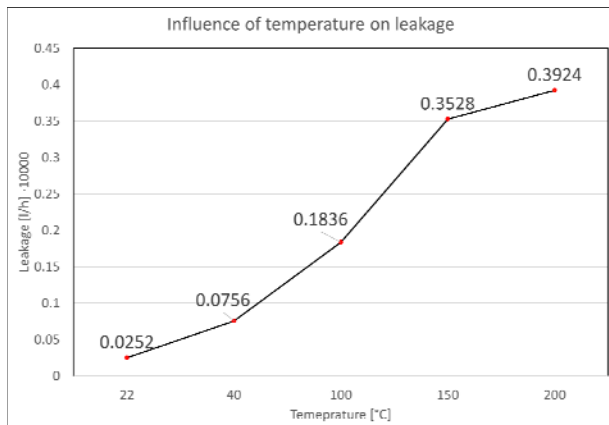
Minimum	0. MPa
Maximum	8.741 MPa
Average	0.41812 MPa

Figure 36. Contact pressures for a process fluid temperature of 200°C

Table 8. Contact pressure comparison

Temperature [°C]	Minimum contact pressure [MPa]	Average Contact pressure [MPa]	Maximum contact pressure [MPa]
22	0.0897	0.22579	0.36202
40	0	0.26233	1.7279
100	0	0.30834	4.7279
150	0	0.36006	6.7346
200	0	0.41812	8.741

Considering the values from table 8, we can see directly the impact of the temperature on mechanical seal contact pressures. With a thin contact surface between the two rings, an increase of leakage will appear, as the non-uniform wear period kicks in. This leakage has been calculated with the support of Ansys Fluent, taking the gaps from the thermal - static calculation, and including them on CFD, doing the same calculation as above. Based on (18), the flow considered is laminar, with a mesh of 0.3 μm (maximum converged by the software). The solution has been considered converged, when the residual values had a value equal with 10^{-6} . Geometries considered for the analysis are the gaps created by the deformation of the rings from figures 29-33. The results are showed in figure 37.

**Figure 37. Influence of temperature on leakage**

The leakage is directly influenced by the gap between the two mechanical seal faces [20]. With increase in deformation, the faces are opening, the interstitial pressure increases inside the opening, and the leakage is increasing. The leakage increase is around ~15 times more, between having an ambient temperature for the process fluid and having 200°C. This increase in temperature will also be dangerous for mechanical seals, as the carbon impregnated material is having a recommended temperature used of maximum 160 - 260°C, depending on the bond and manufacturer. Considering the fact that the mechanical seal is unbalanced, this will also diminish the temperature range that the seal can operate in.

5. CONCLUSION

The paper presents a mathematical model for a CDSA mechanical seal, that has been validated using the API 682 [9]. A discrepancy of maximum 6,6% was obtained, mainly due to materials deformations, as the standard

considers the materials being perfectly rigid, which is not correct. FEA simulations presented have shown this behavior. On the stand-by calculation done, the difference between analytical and FEA model, was close to none, but with each iteration, when a new load was added that deforms the mechanical seal, the difference increases.

The calculation can be used to understand the sensibility of a mechanical seal when it comes to temperature, as a low temperature increase, of 18°C (see the case of process fluid at 22°C and 40°C), can increase the leakage by 3 times.

The analysis is focusing on reverse engineering and existing mechanical seal, type CDSA, and calculates the behavior under different temperatures of the process fluid, under the following assumptions:

- The radiation heat transfer was ignored;
- The temperature distribution on the mechanical seal does not change in time;
- The convection value for air was considered as 0;
- The minimum gap between the two faces will always be equal to the roughness calculated by (19).

With the calculation finalized, the results showed an increase opening on the mechanical seal interstitial, due to thermal deformation (when the process fluid temperature is equal with 200°C), up to 6 μm , resulting in a leakage increase of more than 15 times, compared with the ambient temperature. This opening is mainly due to temperature increase on the outer surfaces of the mechanical seal 316L SS body, that is deforming the mechanical seal, together with the effects of internal and external pressure, but also spring force and rotational velocity.

Due to above mentioned deformation, the seal increased contact pressure, will generate more heat between the two contact faces, including wear, resulting in potential failure. To eliminate this situation, some manufacturers are preparing the exterior layers with a thin extrusion, to compensate for the deformation.

Other solutions for lowering the thermal deformation will be to use another type of material instead of 316L SS, to use a barrier fluid with a lower temperature, or to use a fluid with a higher convection coefficient for the heat transfer.

NOMENCLATURE

H	Seal face generated heat power
T_r	Running torque
N	Rotation per minute
D_m	Mean face diameter
f	Friction coefficient
A	Contact face area
D_o	Outside diameter
D_i	Inside diameter
p_c	Contact pressure
Δp	Pressure across the seal face
K	Pressure drop coefficient
p_{sp}	Spring pressure
B	Seal balance ratio
D_b	Balancing diameter
F_t	Total force acting on a mechanical seal

F_h	Hydraulic force acting on the mechanical seal
F_c	Friction force between the O-Rings and mechanical seal rings
F_{sp}	Total spring force
f_c	friction coefficient
L	Length of seal rubbing surface
C	Seal Compression
A_0	O-ring diameter
A_d	Deformed O-ring diameter
k	Spring constant
x	Spring displacement
G	Shear modulus
d	Spring wire diameter
N_s	Number of spires
R	Average radius of the spring
D_{sp}	Spring diameter
k_f	Thermal conductivity coefficient of sealed medium
P_r	Prandtl number of sealed medium
D_r	Periphery equivalent diameter of rotating ring
ν	Kinematic viscosity of sealed medium
U	Axial velocity of the sealed medium around rotating ring
S_s	Clearance between the peripheral cylinder surface of stationary ring and inner cylinder surface of shell
V	Axial velocity of the sealed medium around stationary ring
Re	Reynolds number
L_w	Characteristics length of the wetted vertical faces of seal ring
V_v	Circumferential velocity of medium in the clearance between two adjacent wetted vertical faces of seal rings
S_v	Clearance between two adjacent wetted vertical faces of seal rings
w	Wear material surplus
x_w	Minimum spring tightening
$F_{sp,l}$	Force per one spring unit
$F_{sp,l,f}$	Force per one spring unit, considering wear
$F_{sp,f}$	Total minimum spring force required
R_c	Total roughness
R_p	Primary ring roughness
R_m	Mating ring roughness

Greek symbols

ω	Rotation speed of the shaft
μ	Dynamic viscosity of the sealed medium
ρ	Density of sealed medium

Superscripts

CDSA Cartridge double seal arrangement

REFERENCES

- [1] Dietzel W., Vasko J.: The evolution and application of mechanical seal face materials, in: *44TH TURBOMACHINERY & 31ST PUMP SYMPOSIA, Engineering Experiment Station*, September 14-17 2015, Huston, Texas <https://hdl.handle.net/1969.1/162203>.
- [2] Gidden A.: *Experimental Analysis of Mechanical Seal Design with Enhanced Thermal Performance*, Master thesis, Louisiana State University and Agricultural and Mechanical College, Louisiana, 2006.
- [3] Etsion I., Kligerman Y., Halperin G., Analytical and Experimental Investigation of Laser-Textured Mechanical Seal Faces, *Tribology Transaction*, 42 (3), pp 511-516, July 1999.
- [4] Q Yu X., He S., Cai R. L.: Frictional characteristics of mechanical seals with a laser-textured seal face, *Journal of Material Processing Technology*, 129 (1), pp. 463-466, October 2002
- [5] [https://doi.org/10.1016/S0924-0136\(02\)00611-8](https://doi.org/10.1016/S0924-0136(02)00611-8).
- [6] Chauhan L. and Duran S.: CFD Investigation Of Mechanical Seal For Improve Thermal Property By Using Different Composite Material In Mating Ring, *International Journal Of Research In Engineering And Technology*, 2321-7308, Vol. 4, May 2015.
- [7] Ahmad N. A., et al., Double Diffusion in Square Porous Cavity Subjected to Conjugate Heat Transfer, *FME Transactions*, Vol. 48, No. 4, pp. 841-848, 2020.
- [8] Ramaganesh R., Subramanian B., Sriram G., Arumugam S. and Ramachadran M., Finite Element Analysis of a Journal Bearing Lubricated with Nano lubricants, *FME Transactions*, Vol. 48, No. 2, pp. 476-481, 2020.
- [9] <https://www.aesseal.com/>, accessed at 28.12.2023.
- [10] API Standard 682, 2014, *Pumps—Shaft Sealing Systems for Centrifugal and Rotary Pumps*.
- [11] Pana I., Preda I.,: *Mechanical seals* (in Romanian), Ed. University of Petroleum and Gas, Ploiesti, 2002.
- [12] <https://www.parker.com/us/en/home.html>, accessed at 22.12.2023.
- [13] Hu Q, Sun J, Ma C., Mechanical Engineering, Thermomechanical coupled analysis of split mechanical seal under different rotation speeds, in: *Advances in Mechanical Engineering*, Volume 8, Issue 12, 2016, <https://doi.org/10.1177/1687814016679565>.
- [14] Chen H.L., Xu C., Zhuo M. Z. and Wu Q.B., The thermal and mechanical deformation study of upstream -pumping mechanical seal, in: *IOP Conf. Ser. : Mater. Sci. Eng*, Volume 72, Issue 4, 042032, 2015, <https://doi.org/10.1088/1757-899X/72/4/042032>.
- [15] <https://www.ansys.com/products/3d-design/ansys-discovery>, accessed at 28.12.2023
- [16] https://www.engineeringtoolbox.com/gasoline-density-specific-heat-dynamic-kinematic-viscosity-thermal-conductivity-vs-temperature-d_2224.html#gsc.tab=0, accessed at 10.01.2024.
- [17] S. Shankar and P. Krshna Kumar: Frictional characteristics of diamond like carbon and tungsten carbide/carbon coated high carbon high chromium steel against carbon in dry sliding conformal contact for mechanical seals, *Mechanics & Industry*

2017, Vol. 8, Issue 115. <https://doi.org/10.1051/meca/2016036>.

- [19] Luan Z., Khonsari M. M., Heat transfer correlations for laminar flows within a mechanical seal chamber, *Tribology International*, Volume 42, No. 5, pp. 770-778, May 2009.
- [20] https://www.sealfaqs.com/?page_id=192#Leakage, accessed at 10.01.2024.
- [21] Ri J. H., Ripeanu R.G., Dinita A., Erosion Modeling in Parallel Gate Valve, *FME Transactions*, Vol. 48, No. 4, pp. 808-815, 2020.
- [22] Stevanovic N. Friction Pressure Loss in micro-channel Rarefied Gas Flows, *FME Transactions*, Vol. 33, No. 2, pp. 65-72, 2005.

**МКЕ АНАЛИЗЕ О УТИЦАЈУ ТЕМПЕРАТУРЕ
ФЛУИДА НА ЦУРЕЊЕ МЕХАНИЧКОГ
ЗАПТИВАЧА**

А. Станчиу, М.Г. Рипеану

Механичка заптивка је динамичка опрема која се састоји од 2 главна дела, статичког прстена и једног ротационог, који такође имају додатне помоћне елементе као што су опруге и заптивке. Ротирајући прстен се гура у контакт трења са статичким прстеном, уз подршку опруга, притиска течности, брзине ротације и других фактора. За минималну вредност цурења, силе које делују на отварање заптивке морају бити мање од оних које га затварају. Механичка заптивка ће увек пропуштати између лица заптивке, јер јој је потребно подмазивање, на основу вредности храпавости. Овај рад показује како температура процесног флуида игра веома важну улогу у одлучивању о понашању механичког заптивача и израчунава цурење на основу различите радне температуре, узимајући у обзир празнину створену термичким ширењем између две стране.